R. & M. No. 2928
(16,141)
A.R.C. Technical Report

MINISTRY OF SUPPLY

AERONAUTICAL RESEARCH COUNCIL
REPORTS AND MEMORANDA

A Detailed Experimental Comparison of Axial Compressor Blades Designed for Free Vortex Flow and Equivalent Untwisted and Twisted Constant Section Blades

By

S. J. Andrews and H. Ogden

LONDON: HER MAJESTY'S STATIONERY OFFICE
1956
PRICE 5*s* 6*d* NET

A Detailed Experimental Comparison of Axial Compressor Blades Designed for Free Vortex Flow and Equivalent Untwisted and Twisted Constant Section Blades

By

S. J. Andrews and H. Ogden

Communicated by the Principal Director of Scientific Research (Air), Ministry of Supply

Reports and Memoranda No. 2928 *
July, 1953

Summary.—As a contribution to the knowledge of the performance of potentially cheap compressor blades, six stages of both twisted and untwisted constant section or ' strip ' blades were tested at a low speed in the 106 compressor. The performance is compared with that of six stages of equivalent free vortex blades, and interstage flow traverses provide the more detailed flow information.

In terms of maximum stage efficiency, the twisted constant section blades are half a per cent better than the free vortex blades and the untwisted blades are one and a half per cent worse. Both twisted and untwisted ' strip ' blades have a higher surge flow than the free vortex blades, but there is very little difference in the temperature rise characteristics. At values of flow coefficient greater than the design flow, the performance of the three sets of blades becomes almost identical and the application of ' strip ' blades at a diameter ratio of 0·75 involves no sacrifice in performance.

Incidental tests on the relation between pressure coefficient and Reynolds number show that the maximum pressure coefficient falls to about half its original value for a change in Re from $1{\cdot}3 \times 10^5$ to $0{\cdot}023 \times 10^5$ and this is accompanied by a reduction in the surge point flow coefficient.

1. *Introduction.*—It has been suggested that a cheap method of making axial compressor blades is to roll or extrude a constant aerofoil section and either braze or weld a root to suitable lengths of the strip. If when building a compressor with this type of blade, the stagger and incidence are chosen to give good two-dimensional performance at the mean blade height, the incidences at both root and tip will be considerably greater or less than those usually designed for. There will also be a variation in work done along the blade span, so that in a multi-stage compressor, the combined effects of variation in work and incidence will distort the velocity profile across the annulus and probably have an adverse effect upon both the efficiency and the surge characteristics of the compressor.

Some of these effects may be avoided by giving the blade a uniform twist from root to tip. If carefully chosen, the twist will produce a variation in stagger which will bring the incidence angles reasonably near the most desirable values over most of the blade length and reduce the design variation in work to negligible proportions.

* N.G.T.E. Report R.141, received 21st September, 1953.

These two types of blade have, in this report, been compared directly with equivalent free vortex blades at low speed in the 106 compressor[1] which has a hub ratio of 0·75. All three blade types were geometrically similar at the mean diameter where the reaction was about 60 per cent. The comparison was, therefore, between :

(i) six stages of untwisted constant section blades (untwisted c.s.),

(ii) six stages of twisted constant section blades (twisted c.s.),

(iii) six stages of free vortex blades,

and from the overall performance of these, the mean stage performance was deduced. To supplement this information, detailed traverses with pitot, static and yaw instruments were made at the first or second and fifth stages. Ref. 3, which is an earlier report relating to part of these investigations, contains some information obtained at a Reynolds number of $1{\cdot}3 \times 10^5$ and some at $0{\cdot}65 \times 10^5$. For the purposes of this report all the tests contained in Ref. 3 have been extended to the higher Reynolds number and re-presented together with the additional tests on twisted constant section blades.

2. *Description of Blading.*—The basis for the design of untwisted, twisted and free vortex blades is the same at mean diameter ; being :

$$\frac{V_{am}}{U_m} = 0{\cdot}66$$

$$\frac{\Delta T_m}{\frac{1}{2}U_m^2} = 0{\cdot}8 \text{ with a work done factor of } 0{\cdot}95.$$

Per cent Reaction = 59·4.

Since the design methods are the same, the blade geometry at mean diameter is identical for rotor and stator blades of the free vortex, untwisted and twisted constant section designs.

It could be argued that the best choice of twist for the twisted constant section blades is that which gives incidence angles nearest the optimum over most of the blade span. There are however an infinite number of possible designs to satisfy the usual assumptions of axial velocity and temperature rise independent of radius, but the three investigated for this purpose were free vortex, constant α_3 and constant reaction. These designs have been found to give satisfactory results in the design of a compressor stage of moderate or high hub ratio, although two of them do not satisfy the criterion for radial equilibrium, *i.e.*, $dp/dr = \rho(V_w^2/r)$.

Of the three, the constant reaction design gave the most reasonable incidences in both rotor and stator, and was therefore adopted. The incidences are shown in Fig. 3 and are compared with the optimum and stalling incidence for the blade section as predicted by Ref. 2. The rotor and stator blades are working below optimum incidence at the outside diameter and above optimum at the inside diameter, but the stalling incidence is not exceeded.

The outlet angles from the untwisted c.s. blades cannot be independently varied so the simultaneous assumption of constant work done and constant axial velocity is not possible. Fig. 3 shows the variation in temperature coefficient and incidence with radius assuming a constant axial velocity, also the variation in axial velocity and incidence assuming constant temperature rise.

In the compressor itself, constant axial velocity might be expected to apply more nearly to the first stage and constant temperature rise to the later stages.

2.1. *Blade Accuracy.*—Although the untwisted and twisted c.s. blades were meant to represent rolled or extruded strip, they were in this instance die cast in light alloy, in exactly the same way as the free vortex blades. All the blades have, therefore, a similar surface finish and manufacturing tolerance.

The accuracy of the blades was estimated by optically projecting samples of six rotor and six stator blades to twenty times full size at the mean diameter section. Taking a mean of the six camber and thickness ratio values for each type of blade, the differences between the actual and design values are shown in the table below :

Blades	Rotor		Stator	
	Camber	t/c ratio	Camber	t/c ratio
Free vortex	26·7	0·103	32·1	0·110
Twisted c.s.	25·0	0·097	33·3	0·107
Untwisted c.s. ..	25·8	0·098	32·6	0·110
Design	26·5	0·100	34·0	0·110

The stagger of the blades was set to an accuracy of $\pm$ 0·1 deg so the worst errors in outlet angle are 0·8 deg in the twisted c.s. rotor blades and 1·0 deg in the free vortex stator blades. Errors of this order are to be expected in any form of cast blade but the difficulty in making a uniform numerical correction to the traverse results is that for the stator rows only one blade is traversed while downstream of the rotor row the traverse is related to every blade in that row. No corrections have been made, therefore, and the results are compared directly with ideal design conditions.

3. *The Compressor and Test Equipment.*—The 106 compressor has a constant rotor and casing diameter, the ratio of the two being 0·75. The rotational speed for those tests other than for Reynolds number effects was 3,000 r.p.m. giving a mean blade speed of 229 ft/sec and Reynolds number, based on this speed, of $1{\cdot}3 \times 10^5$. At these speeds, the maximum density ratio over six stages is about 1·08 and the use of six identical stages in a constant annulus is justified for a comparison of blades having similar overall performance.

A full description of the compressor is given in Ref. 1 and Fig. 1 shows both the construction of the compressor and the arrangements for traversing in a stage. The tip clearances maintained during tests were 0·020 in. to 0·025 in. for the rotor blades and 0·015 in. to 0·020 in. for the stator blades.

3.1. *Instrumentation.*—Measurements made on the compressor were the overall total pressure rise, the mass flow, the input torque of the driving motor, and the static-pressure rise per stage. From these are derived the pressure, temperature and flow coefficients and the isentropic efficiency.

3.2. *Pressure Rise.*—The rise in pressure measured is from inlet total (atmospheric pressure) to the outlet total pressure indicated by two combs of five pitot-tubes. The combs are about two chords downstream of the last stator row and at opposite ends of a diameter. Each tube samples an equal increment of radius and they are yawed in unison to give the maximum value for the arithmetic mean total pressure.

3.3. *Mass Flow.*—The four inlet static-tubes were calibrated against a standard orifice in the outlet duct with a repeatability within 0·5 per cent in mass flow reading.

3.4. *Torque Input.*—The driving motor is mounted on trunnion bearings so the torque measured on its casing is due to the compressor work output, bearing friction and windage. The bearing friction is partly corrected for by taking the torque reading at a series of low speeds and extrapolating to zero speed to obtain the torque reading zero error. The torque value from which the

work done is determined does not therefore include the bearing friction torque at speeds tending to zero. It does include, however, any increase in bearing friction with speed and, of course, windage.

Refinements to the measuring system include motorised contra-rotating outer races for the two trunnion bearings which considerably reduces the hysteresis, and a null movement system for the motor casing torque measurement in order to minimise the stiffness effect of electrical connections. With such a system, repeatability of results is within $\pm$ 0·5 per cent.

3.5. *Stage Pressure Rise and Flow Conditions.*—Between each stage in the compressor stator casing are four surface static-pressure points for finding the pressure characteristic of each individual stage. The traversing instruments are, in order of use, an ' arrow-head ' type pitot yawmeter and a static-pressure tube. The pitot yawmeter is made from three tubes of 0·060 in. outside diameter and the static-pressure instrument of tube 0·040 in. outside diameter.

4. *Comparative Performance of Blades.*—The overall characteristics were obtained for six identical stages of each type of blading and are expressed in Fig. 4 as non-dimensional pressure and temperature rise per stage and isentropic efficiency, against flow coefficient.

The density ratio in the compressor is about 1·08, so the density term in the pressure coefficient must be based on a mean value. This value is the mean of the densities corresponding to total pressure and temperature at inlet and outlet (ρ_M). The method of expression is more convenient than that using true density, both for computation and conversion, should this be necessary, and does not invalidate the comparison. The axial velocity V_{aM}, the numerator of the flow coefficient, is determined from the mean ' total ' density ρ_M and the mass flow.

4.1. *Overall Characteristics.*—The maximum efficiency of the free vortex blades is about 86 per cent (Fig. 4). The maximum efficiency of the twisted c.s. blades is $\frac{1}{2}$ per cent higher and of the untwisted c.s. $1\frac{1}{2}$ per cent lower. There is little difference between the pressure and temperature characteristics, except that, compared with the free vortex blades, the twisted and untwisted c.s. blades surge at a progressively higher flow. This is to be expected since under design conditions the incidence at the inner diameter on the twisted constant section stator blades is within a degree of the stalling incidence, as predicted by the data given in Ref. 2, and the design conditions are even worse at the roots and tips of the untwisted blades.

At flows higher than the design flow, the efficiency curves converge. It is possible, therefore, to use untwisted c.s. blades in the final stages of a multi-stage compressor without sacrifice in efficiency, since the flow coefficient will be greater than the design value for most conditions and the diameter ratio for these tests should be applicable.

The similarity of the characteristics is quite remarkable for blades of such different twist. The implication is that at this diameter ratio, the performance is characterised by the mean diameter sections, with blade twist having only a very secondary effect.

4.2. *Stage Characteristics.*—Individual stage characteristics deduced from static-pressure tappings at the outside diameter between stages are shown in Fig. 5. Other than in the first stages, the characteristics are very similar. The only tendency to serious deterioration from stage to stage is in the last stage of untwisted c.s. blades. At this point the annulus boundary-layer growth coupled with the velocity profile imposed by the variation in work done in the early stages, produces an incidence variation for which both rotor and stator blades are stalled over at least half the blade height.

The first-stage characteristics are steeper than those of the other stages and although similar in shape, are displaced to about the same extent and in the same direction as the surge flows on the overall characteristics. The result is that the maximum pressure coefficient reached in the first stage is about the same for each set of blades. The steepness of the first-stage characteristics is a usual feature of first stage performance where secondary effects are a minimum. It is important to note that the inlet guides used with the untwisted c.s. blades were those specifically designed for the free vortex blade set, *see* Appendix I.

5. *Blade Performance in Detail.*—Interstage flow traverses were made over one blade pitch before and after the first or second and fifth-stage stator blade rows for each set of blades. The traverse instrument arrangement is illustrated in Fig. 1. The disadvantage in doing two instead of three traverses per stage is that in traversing before and after the second stage stator, the α_0 and a_1 are of the third stage, while α_2 and α_3 are of the second stage. Any derived temperature rise, therefore, leads to the method of plotting at half-stage positions as shown in Fig. 14.

The results of these traverses at a constant Reynolds number of $1{\cdot}3 \times 10^5$ are shown in Figs. 6 to 11.

5.1. *Axial Velocity Profiles.*—The axial velocity profiles derived from circumferential mean values for a traverse over one blade pitch are shown in Figs. 6 and 7. The velocity distribution for the untwisted c.s. blades is compared with the distribution necessary for constant work over the blade height given in Fig. 3 and in the second-stage stator row, this distribution is achieved within the limits imposed by the boundary-layer growth.

Comparing the velocity profiles in the fifth stage of each set of blades, it is evident that the twisted c.s. blades cause the least deterioration. This is illustrated further in Fig. 14. The basis for comparison in this figure is the velocity profile assumed in design, but since the untwisted c.s. blades have no design assumptions, the design velocity distribution for these blades is taken as that required to give constant work. It is for this reason that in Fig. 14 the curve corresponding to the untwisted c.s. blades does not begin at the origin, since a constant axial velocity represents a considerable deviation from the ' design ' value.

The rate of deterioration of the velocity profile in the last few stages of both free vortex and twisted c.s. blades is almost negligible. The untwisted blades, however, have a marked velocity profile deterioration consistent with the variation in stage characteristics.

An interesting effect noticeable in Fig. 14 is the apparent improvement in the velocity profile in passing through a stator row.

5.2. *Radial Equilibrium.*—At each traverse position both gas angles and total pressures are measured. For these measured values there is, as shown in Ref. 6, only one distribution of axial velocity for which, assuming zero radial flow, there is radial equilibrium. These axial velocities were calculated for the measured total head and gas-angle distributions and compared with the experimental values. From Figs. 8, 9, 10 and 11, it is evident that this radial equilibrium is largely satisfied at all traverse positions for free vortex, twisted and untwisted c.s. blades. In view of past experience (Ref. 5), this is surprising since the spacing of the blade rows is only two-thirds of a chord and the traverse plane is less than half-a-chord down-stream of the trailing edges.

5.3. *Gas Angles.*—The gas angles for first or second and fifth stages are shown in Figs. 8, 9, 10 and 11. It would be confusing to give in detail the full picture as shown by these results, but there are a few points of particular interest.

The stator blades have deviation angles which are up to three degrees greater than would be predicted by data in Ref. 2 even though the incidences are much lower than the predicted stalling incidence. The measured loss coefficients in the stators are not completely reliable but it seems that the high deviation is not associated with a high loss-coefficient and is not, therefore, due to serious separation. The stators also show signs of secondary effects in the final stages. At the inner diameter of the fifth stage the deviation is maintained at a low value, although the blade is working above stalling incidence. Towards the outer diameter, however, the deviation increases rapidly while the incidence, although increasing, is still below the design value.

Except in the first stage of untwisted c.s. blades, the rotor gas outlet angles conform to the design rule over the range of incidence where this agreement can be expected. The variation in work done in the first stage of untwisted c.s. blades, Fig. 9, is not of the same order as that theoretically produced by a constant axial velocity. Judging, however, by the rapidly changing velocity profile in the first stator, Fig. 6, the condition in the first stage represents an intermediate state between constant axial velocity and constant work-done conditions.

5.4. *Work-Done Factor.*—The true work done in the rotor blade row is obtained by integrating the angular momentum per second across the annulus and taking the difference of the integrals at inlet and outlet. This value is compared with that using design gas angles and velocities and the ratio of the two is the work-done factor, the variation of which is illustrated in Fig. 14.

$$\Omega = \frac{\left[\int_{r_i}^{r_o} UV_{a2}^2 \tan \alpha_3 r\, dr - \int_{r_i}^{r_o} UV_{a1}^2 \tan \alpha_0 r\, dr\right]}{\left[\int_{r_i}^{r_o} UV_{a2}^2 \tan \alpha_3 r\, dr - \int_{r_i}^{r_o} UV_{a1}^2 \tan \alpha_0 r\, dr\right]} \quad \begin{matrix}\text{actual} \\ \text{design}\end{matrix}$$

The inference from Fig. 14 is that the work-done factor may be high in the first stage but remains about constant in subsequent stages at a value lower than that usually assumed. This variation follows the same pattern as for axial velocity profiles and stage pressure characteristics.

6. *Reynolds Number Effects.*—Reducing the speed of the compressor and using a micromanometer, the Reynolds number was reduced to a minimum of 2,300. The effect upon pressure coefficient is illustrated in Figs. 12 and 13. There is evidently some critical Reynolds number between 3,000 and 4,000 where the surge flow coefficient begins to decrease rapidly as the Reynolds number is reduced.

For all sets of blades, the relation between maximum pressure coefficient and Reynolds number is approximately a one-fifth power law, Fig. 13.

$$\frac{\Delta P}{\frac{1}{2}\rho U_m^2} \propto (Re_U)^{1/5}.$$

This does not correspond to the widely used rule

$$(1 - \eta) \propto (Re_U)^{-1/5}$$

but for these tests no confirmation or otherwise of the rule was obtained because it was quite impossible to measure the low torque values from which the efficiency could be derived at these low speeds.

7. *Conclusions.*—In an axial compressor of diameter ratio 0·75 untwisted constant section or ' strip ' blades will, at a high flow coefficient, yield as good a performance as equivalent conventional free vortex blades. The untwisted constant section blades are, however, working near the limit of velocity profile which they will accept without excessive stalling at the inner diameter. The twisted constant section blades show least susceptibility to stalling near the blade root and tip radii, being in fact slightly better even than the free vortex blades. Furthermore the twisted constant section blades have a rate of deterioration of flow conditions through several stages which is less than that of the free vortex blades.

Both twisted and untwisted constant section blades have a surge flow a little higher than the free vortex blades, but, apart from this, the use of the twisted constant section blades involves no sacrifice in performance at low Mach numbers and may result in a slight gain.

In the 106 compressor, the variation of maximum pressure coefficient with Reynolds number based on blade speed, is according to a one-fifth power law.

Acknowledgment.—The authors are indebted to Miss J. Marshall for the valuable assistance in computation and analysis of results.

REFERENCES

No.	Author	Title, etc.
1	R. A. Jeffs	Description of the low speed experimental compressor (No. 106). Power Jet Report R.1198. A.R.C. 6842. April, 1946.
2	A. D. S. Carter	The low speed performance of related aerofoils in cascade. C.P. 29. September, 1949.
3	S. J. Andrews and H. Ogden	A detailed experimental comparison of blades designed for free vortex flow and equivalent untwisted constant section blades. N.G.T.E. Report R.123. A.R.C. 15,328. August, 1952. (To be published.)
4	S. J. Andrews and E. L. Hartley ..	A detailed experimental comparison of axial compressor blades designed for free vortex flow and blades designed for increased work at root and tip. N.G.T.E. Report R.104. A.R.C. 14,671. October, 1951. (To be published.)
5	D. G. Ainley and R. A. Jeffs	Analysis of air flow through four stages of half vortex blading in an axial compressor. R. & M. 2383. April, 1946.
6	A. D. S. Carter	Vortex wind tunnel tests on various vortex flows. Power Jet Report R.1063.

NOTATION

U	Blade speed
V_a	Axial velocity
r	Radius
ΔT	Total temperature rise
ΔP	Total pressure rise
ρ	Density
s	Blade pitch
c	Blade chord
ε	Gas deflection angle
ζ	Blade stagger angle measured from axial direction
α	Gas angle measured from axial direction
β	Blade angle measured from axial direction
Ω	Work done factor
$\bar{\omega}$	Mean total pressure loss
η	Isentropic efficiency
Re_U	Reynolds number based on mean blade speed U_m

Suffixes

0	After stator row of previous stage
1	Before rotor blade row
2	After rotor blade row
3	Before stator blade row
4	After stator blade row
m	Mean annulus diameter
M	Mean of compressor inlet and outlet conditions
R	Rotor
S	Stator

APPENDIX I

Design of Free Vortex Blades

Assumptions :

$$V_a = \text{constant}$$

$$\frac{U_m}{V_a} = 1{\cdot}5$$

$$\frac{\Delta T}{\frac{1}{2}U_m^{\,2}} = 0{\cdot}8 \text{ including work-done factor } \Omega$$

$$\Omega = 0{\cdot}9$$

$$\text{Reaction} = 50 \text{ per cent at } \frac{r}{r_m} = 0{\cdot}9$$

$$\tan_3 \propto \frac{1}{r}$$

$$\tan_0 \propto \frac{1}{r} \quad .$$

The temperature rise at radius r is :

$$\frac{\Delta T}{\frac{1}{2}U_m^{\,2}} = 2\frac{V_a}{U_m}\frac{r}{r_m}\,(\tan\alpha_3 - \tan\alpha_0)\Omega$$

$$= 1{\cdot}27\,\frac{r}{r_m}\,(\tan\alpha_3 - \tan\alpha_0).$$

At the radius for 50 per cent reaction $\left(\frac{r}{r_m} = 0{\cdot}9\right)$

$$\tan\alpha_3 - \tan\alpha_0 = \frac{U_m}{V_a}\frac{r}{r_m} = 1{\cdot}35.$$

The design gas angles are therefore :

r (in.)	7·5	8·12	8·75	9·37	10·0
r/r_m	0·86	0·93	1·0	1·07	1·14
α_1	43·6	47·3	50·4	53·1	55·5
α_2	12·3	22·0	30·0	36·6	42·0
α_3	47·0	44·7	42·7	40·8	39·0
α_4	18·6	17·3	16·2	15·2	14·3

Design of Twisted Constant Section Blades

Assumptions :

$$V_a = \text{constant}$$

$$\frac{U_m}{V_a} = 1{\cdot}5$$

$$\frac{\Delta T}{\frac{1}{2}U_m^2} = 0{\cdot}8 \text{ including work-done factor.}$$

All blade details at the mean diameter are identical to those at the mean diameter of the free vortex blades which means that :

$$\text{Reaction} = 59{\cdot}4 \text{ per cent at } r/r_m = 1{\cdot}0$$

A uniform strip of aerofoil section corresponding to the mean diameter can be twisted so that the outlet gas angles correspond to any arbitrarily selected design rule, but the incidence will only be correct at mean diameter. Of the three considered, free vortex, constant α_3 and constant reaction, the most reasonable incidences were those for a constant reaction design of 59·4 per cent, so with this criterion :

$$\tan \alpha_3 + \tan \alpha_0 = 2(1 - 0{\cdot}594)\frac{U}{V_a}$$

$$\tan \alpha_3 + \tan \alpha_0 = 1{\cdot}368\, r/r_m .$$

Then for the constant temperature rise

$$\tan \alpha_3 - \tan \alpha_0 = \frac{2}{\Omega}\left(\frac{\Delta T}{\frac{1}{2}U_m^2}\right)\frac{U_m}{U}\frac{U_m}{V_a}$$

$$= 0{\cdot}632\, r/r_m$$

which gives gas angles of :

r (in.)	7·5	7·87	8·75	9·37	10·0
r/r_m	0·86	0·90	1·0	1·07	1·14
α_1	48·6	49·1	50·4	51·3	52·2
α_2	21·8	24·2	30·0	33·3	36·5
α_3	41·7	42·0	42·7	43·5	44·1
α_4	8·9	11·1	16·2	19·6	22·8

Design of Untwisted Constant Section Blades

The untwisted constant section blades have blade sections identical with those at mean diameter of both free vortex and twisted constant section blades.

r (in.)	7·5	8·12	8·75	9·37	10·0
r/r_m	0·86	0·93	1·0	1·07	1·14
α_1	Constant V_a or constant work (*see* Fig. 3)				
α_2	29·4	29·7	30·0	30·2	30·4
α_3	—	—	—	—	—
α_4	15·7	16·0	16·2	16·5	16·9

Blade Angles

Blade angles are fitted to the gas angles by the deviation rule $m\theta\sqrt{(s/c)}$ (Ref. 2) and for the free vortex blades, a similar incidence rule. The angles of the twisted c.s. blades are modified by a very small amount to linearise the twist.

Free vortex

r/r_m	0·86	1·00	1·14
β_1	43·9	49·5	52·3
β_2	2·9	23·0	37·4
β_3	47·5	42·4	37·5
β_4	9·8	8·4	6·4

Twisted constant section

r/r_m	0·86	1·00	1·14
β_1	43·0	49·5	55·9
β_2	16·5	23·0	29·4
β_3	36·2	42·4	48·8
β_4	2·2	8·4	14·8

Untwisted constant section

r/r_m	0·86	1·00	1·14
β_1	49·5	49·5	49·5
β_2	23·0	23·0	23·0
β_3	42·4	42·4	42·4
β_4	8·4	8·4	8·4

Fig. 3 gives the t/c, s/c and chord of the blades at each radius.

The inlet guide blades designed for the free vortex blades were used also for the untwisted constant section blade tests.

Inlet Guide Vanes

Free vortex and untwisted c.s.			
r/r_m	0·86	1·00	1·14
β_1	−1·1	−3·7	−6·4
β_2	−22·1	−19·2	−16·4

Twisted c.s.			
r/r_m	0·86	1·00	1·14
β_1	+7·2	0	−7·2
β_2	−12·6	−19·8	−27·0

The thickness, chord and pitch for the blades are similar to the figures for the stator blades (*see* Fig. 3).

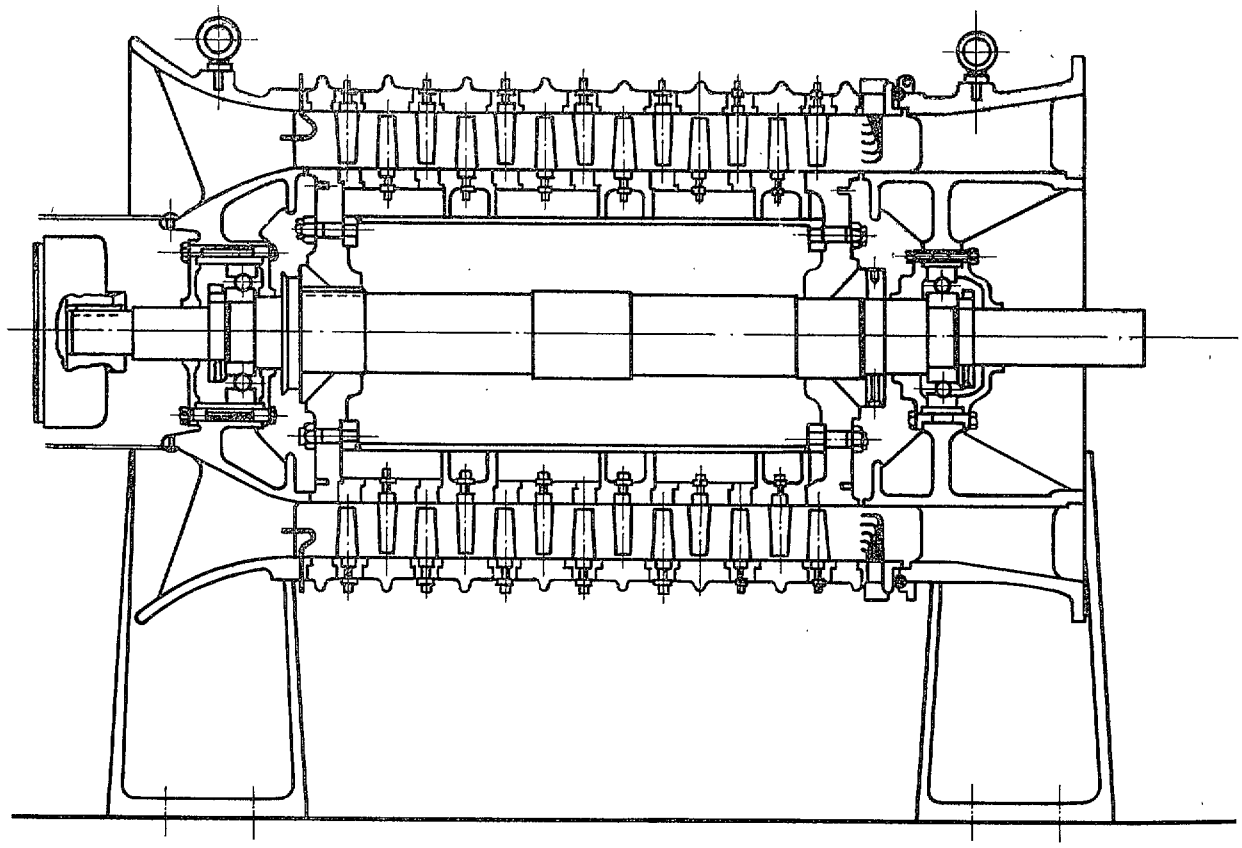

Compressor construction.

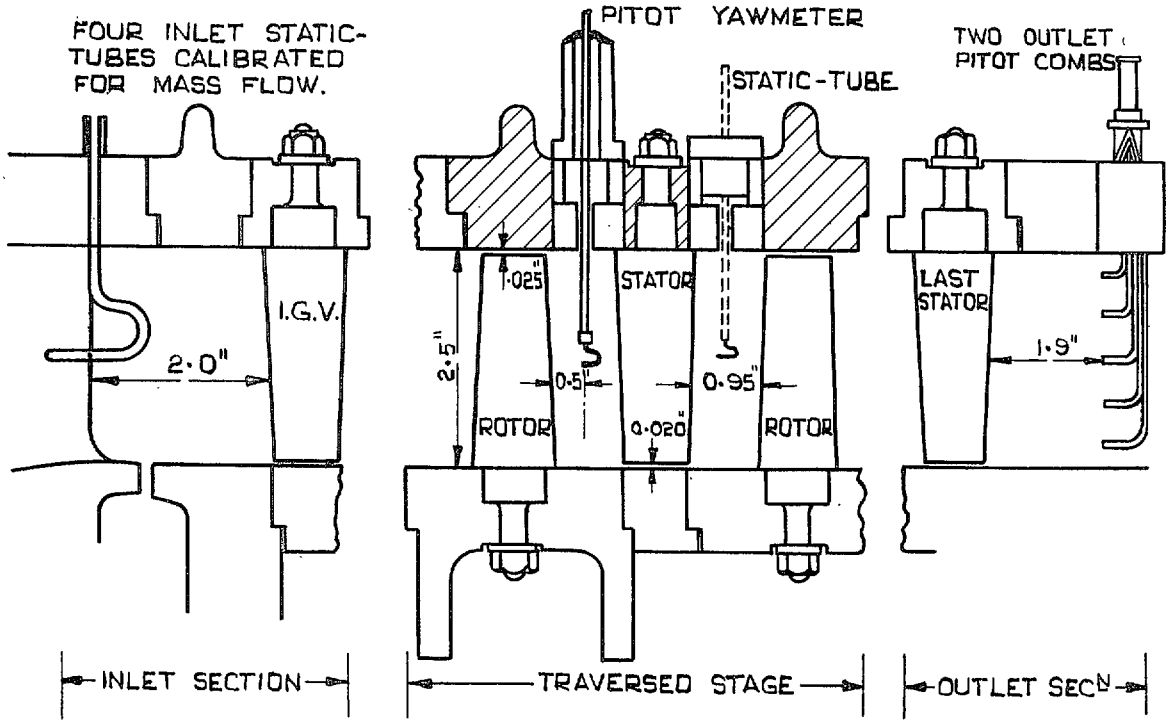

Instrumentation.

FIG. 1. The 106 low-speed compressor.

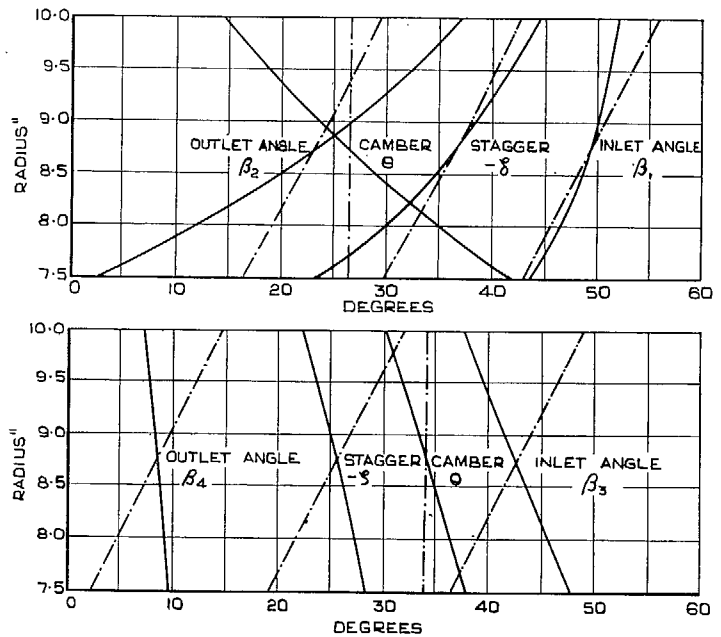

	OUTLET ANGLE	STAGGER	CAMBER	INLET ANGLE
ROTOR	23·0	−36·3	26·5	49·5
STATOR	8·5	−25·5	34·0	42·5

FREE VORTEX T.C.S. AND U.C.S.

RADIUS	7·50"		8·75"		10·0"		ALL RADII	
	R	S	R	S	R	S	R	S
CHORD	1·14	1·06	1·10	1·10	1·06	1·14	1·10	1·10
PITCH/CHORD	·711	·738	·862	·832	1·040	·918	α +	
THICK/CHORD	·120	·100	·100	·110	·080	·120	·100	·110
NUMBER BLDS	58	60	—	—	—	—	58	60

FIG. 2. Blade angles and data for the three sets of blades.

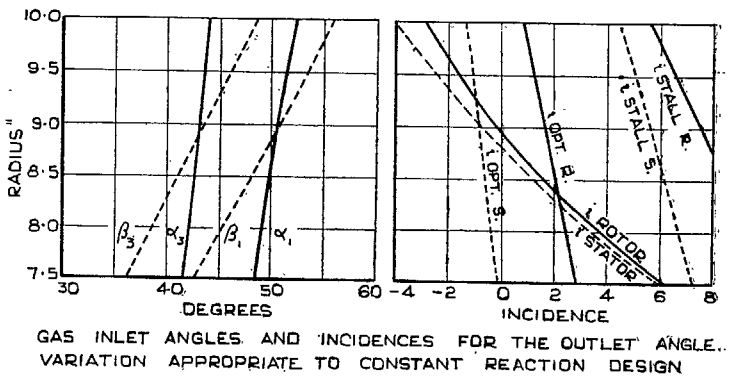

GAS INLET ANGLES AND INCIDENCES FOR THE OUTLET ANGLE VARIATION APPROPRIATE TO CONSTANT REACTION DESIGN

Twisted constant section.

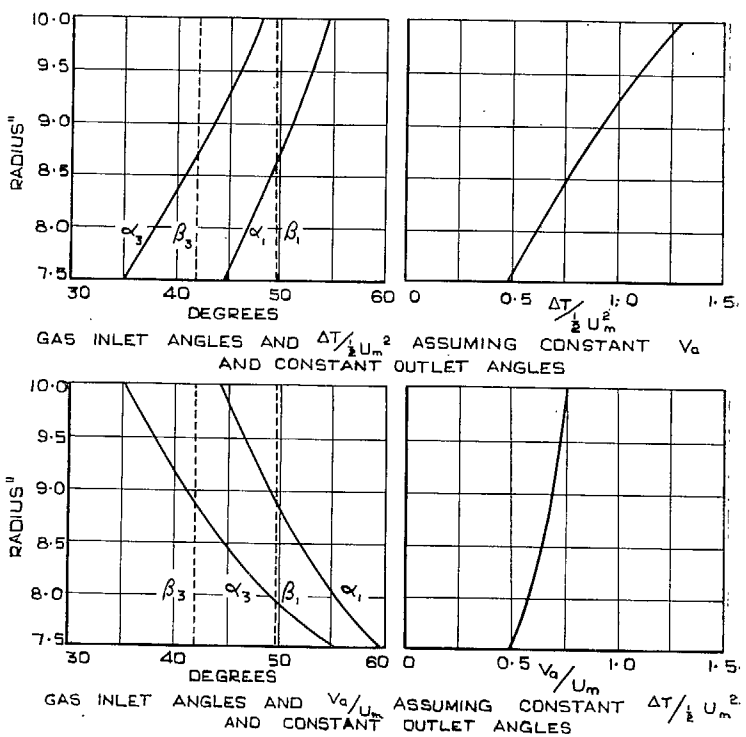

GAS INLET ANGLES AND $\frac{\Delta T}{\frac{1}{2}U_m^2}$ ASSUMING CONSTANT V_a AND CONSTANT OUTLET ANGLES

GAS INLET ANGLES AND $\frac{V_a}{U_m}$ ASSUMING CONSTANT $\frac{\Delta T}{\frac{1}{2}U_m^2}$ AND CONSTANT OUTLET ANGLES

Untwisted constant section.

FIG. 3. Variations from conventional design conditions.

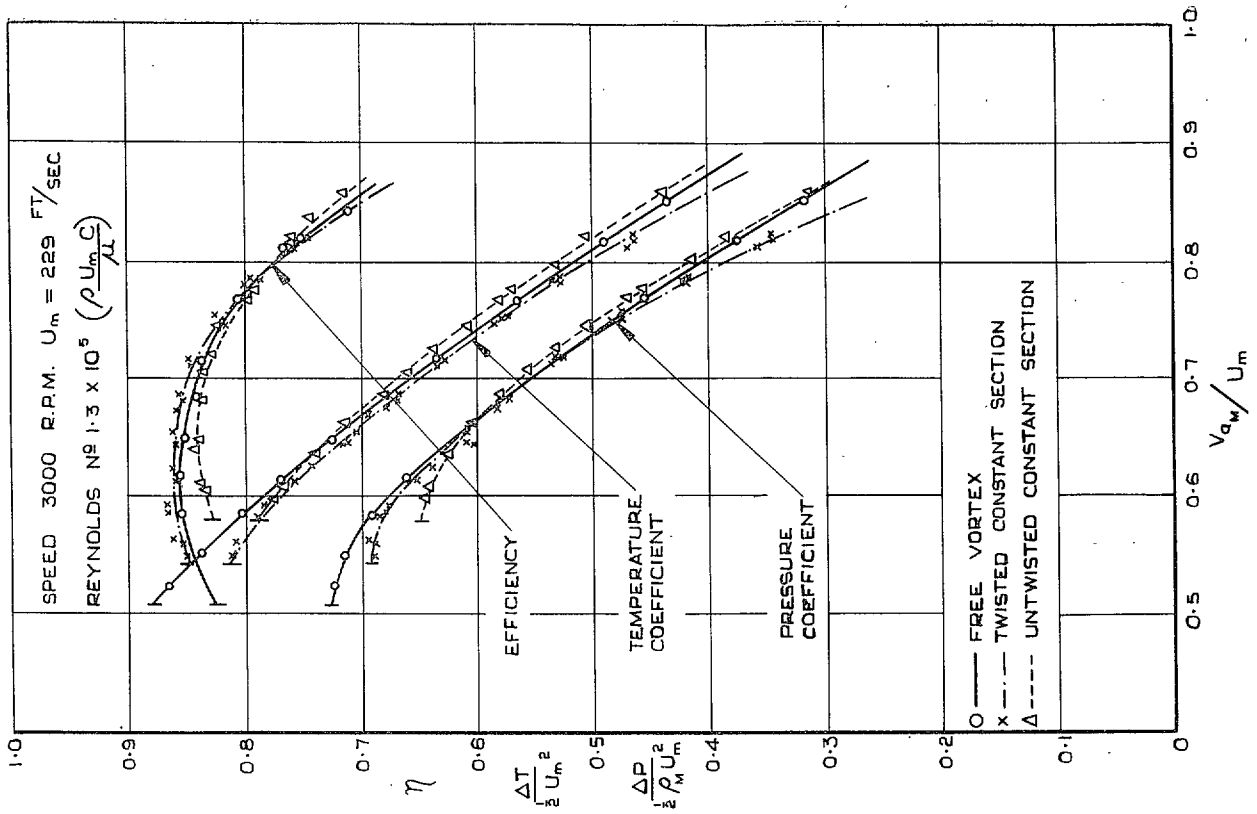

FIG. 4. Overall compressor characteristics.

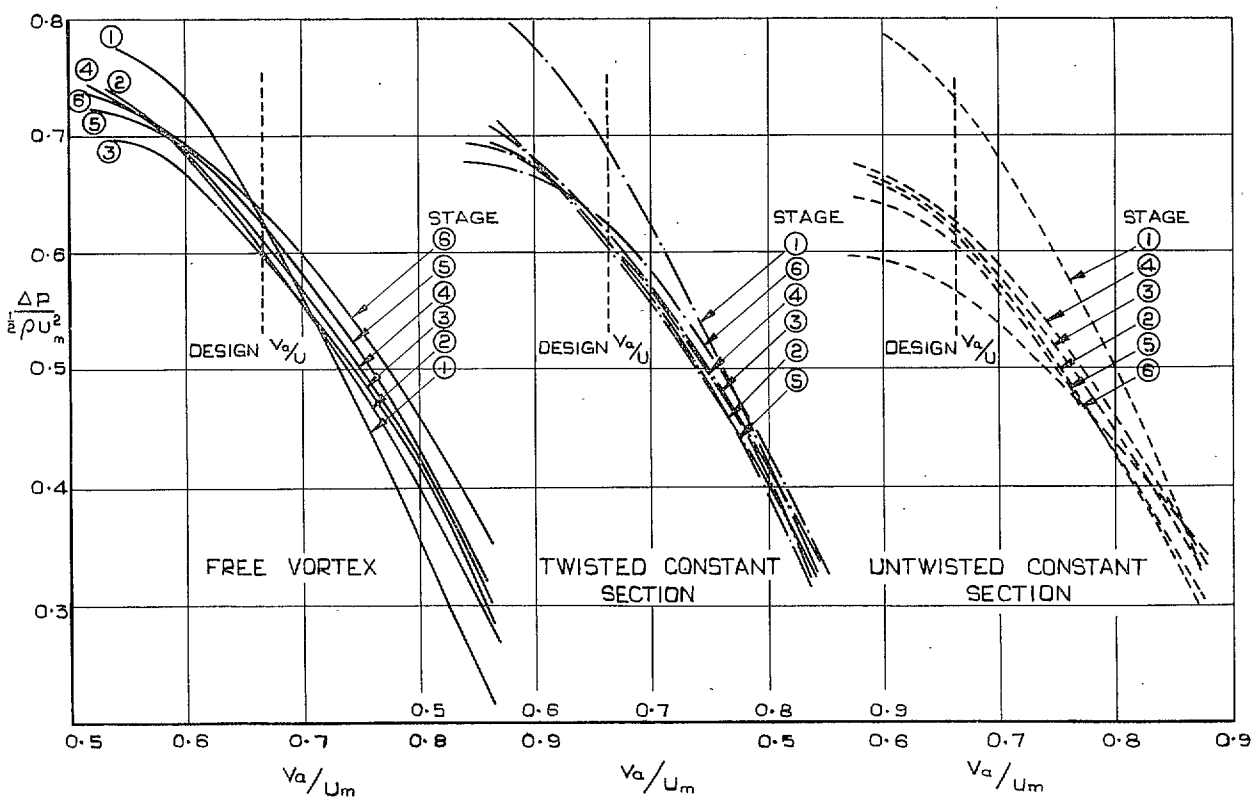

FIG. 5. Compressor stage characteristics.

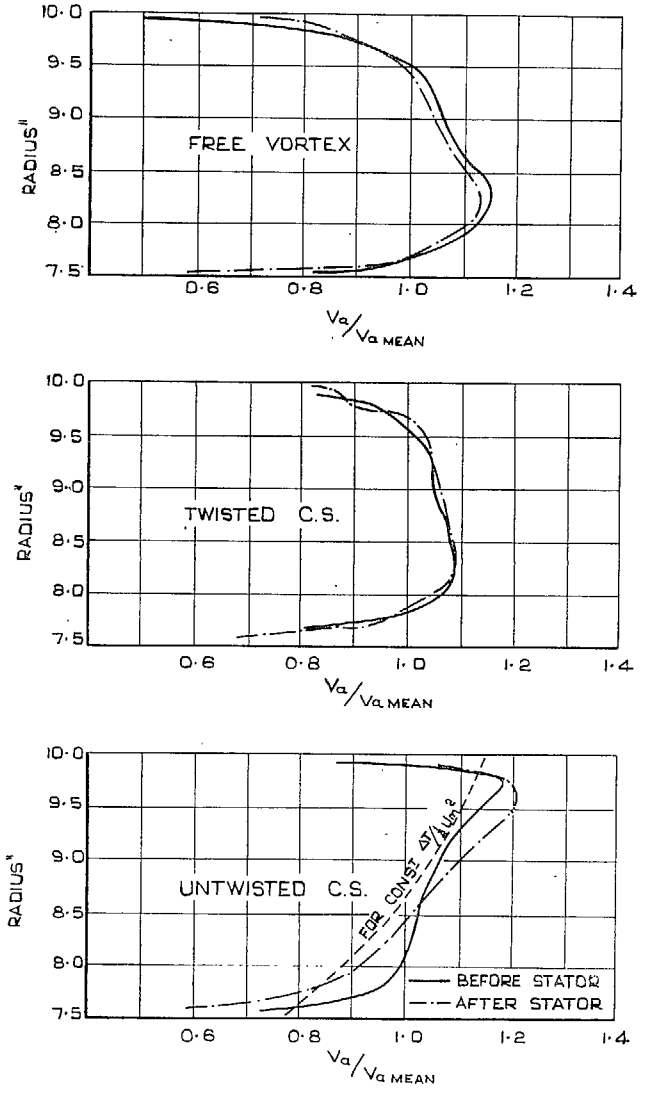

FIG. 6. Circumferential mean axial velocity profiles. Second stage.

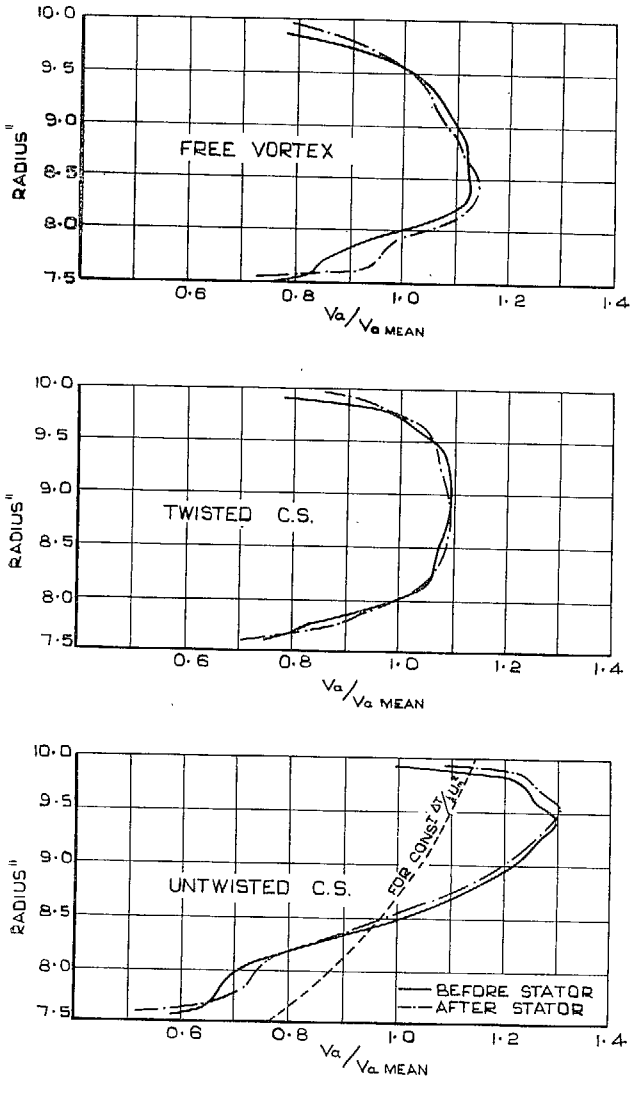

FIG. 7. Circumferential mean axial velocity profiles. Fifth stage.

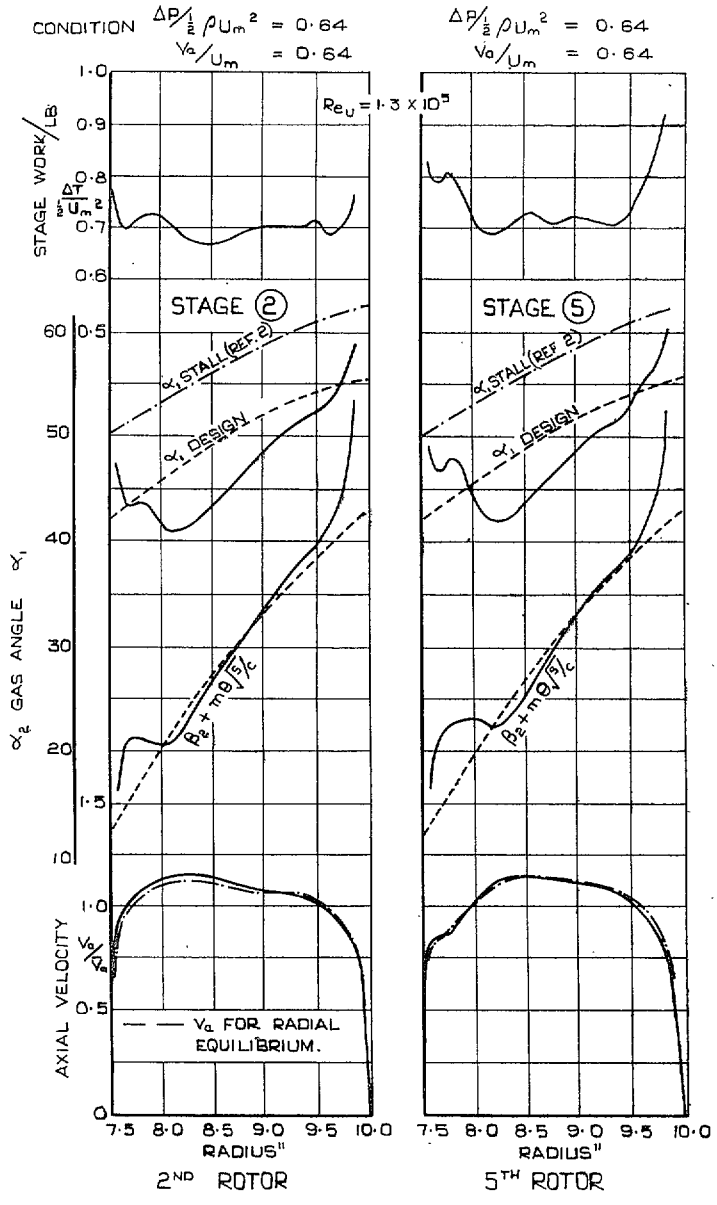

FIG. 8. Free vortex blades.

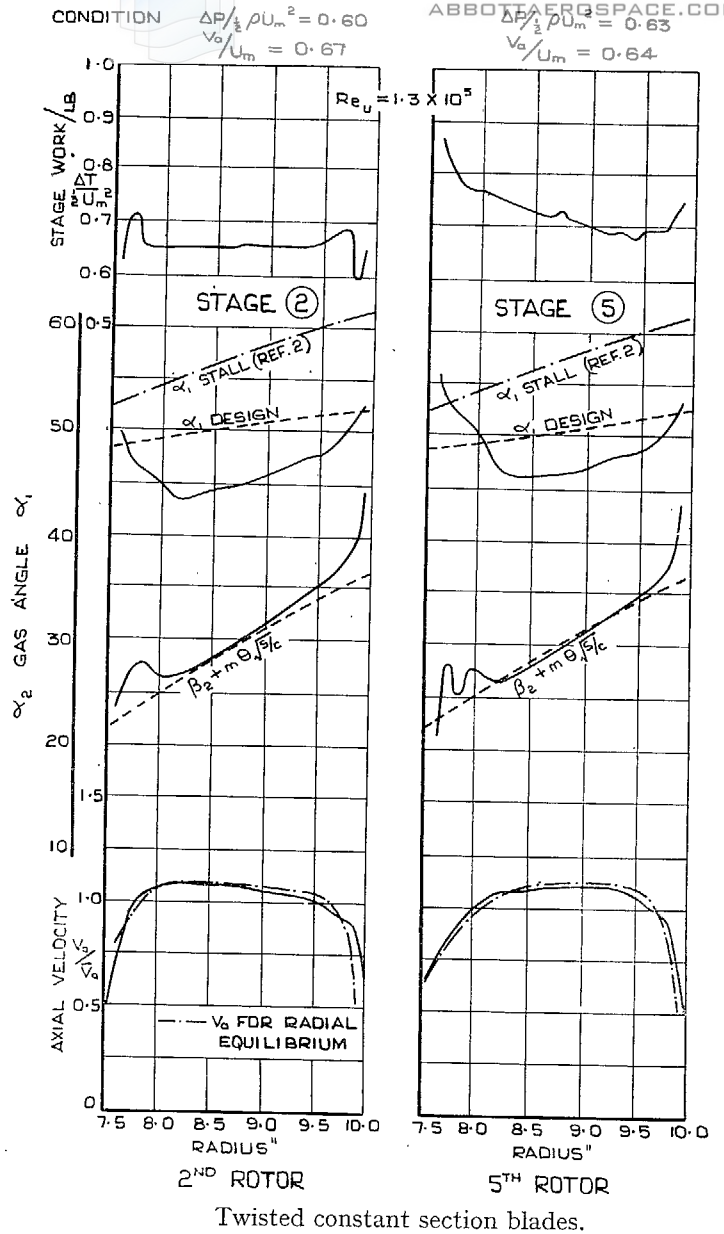

Twisted constant section blades.

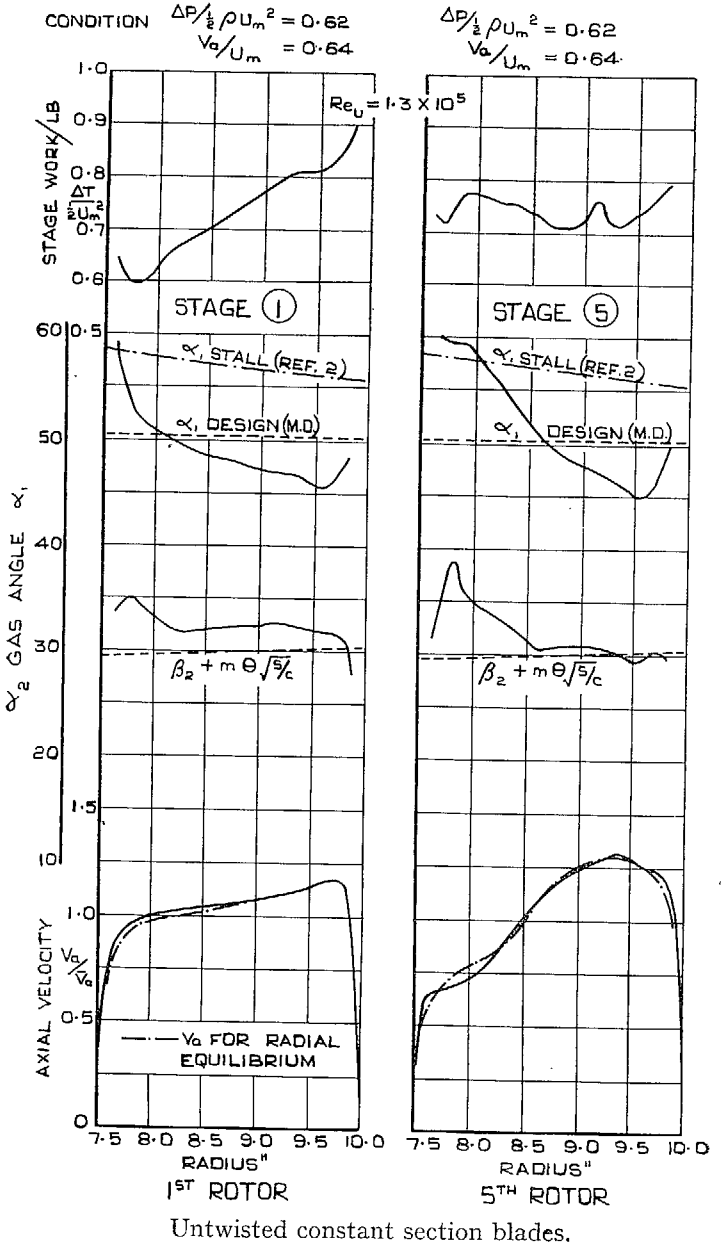

Untwisted constant section blades.

FIG. 9.

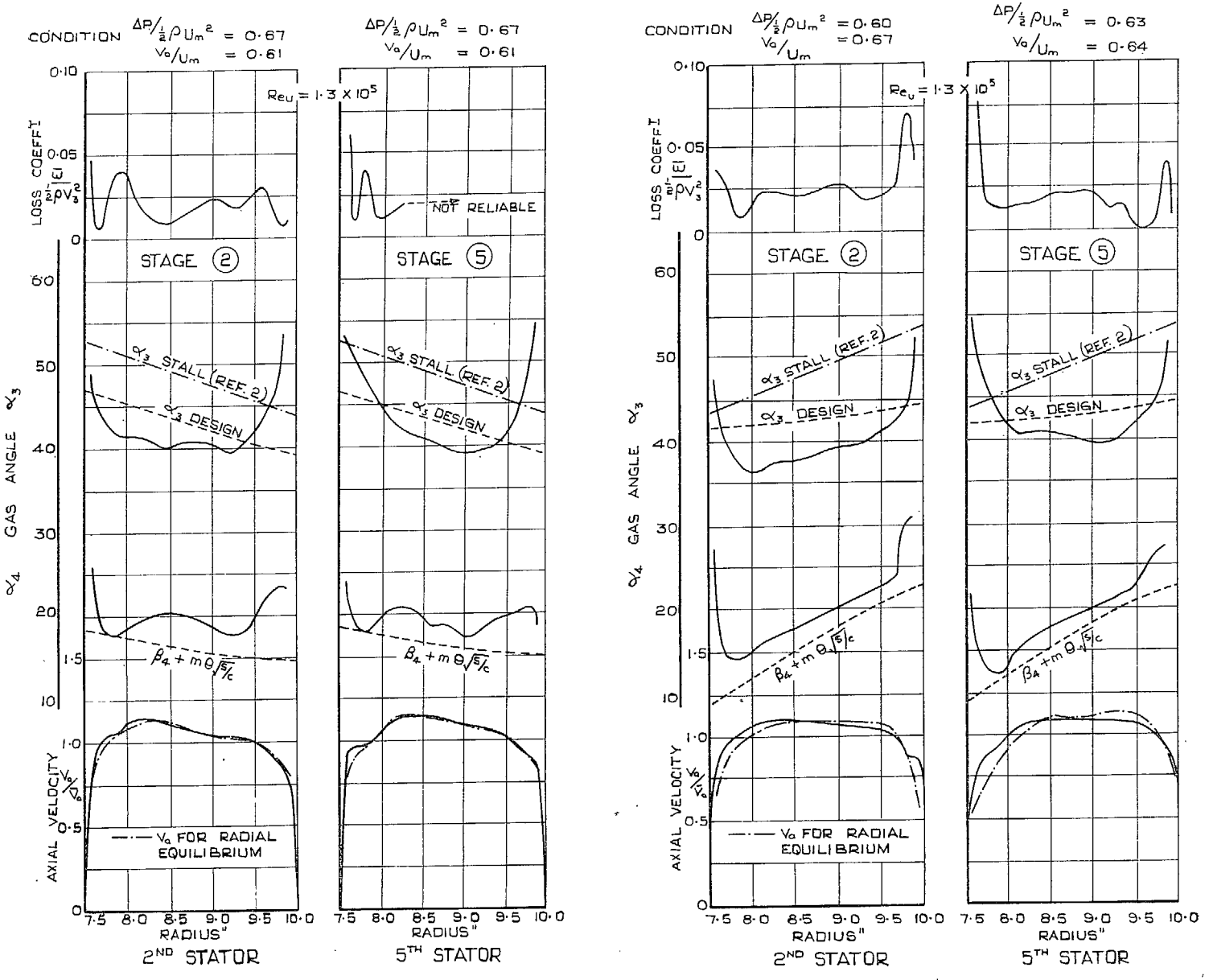

Free vortex blades.

Twisted constant section blades.

FIG. 10.

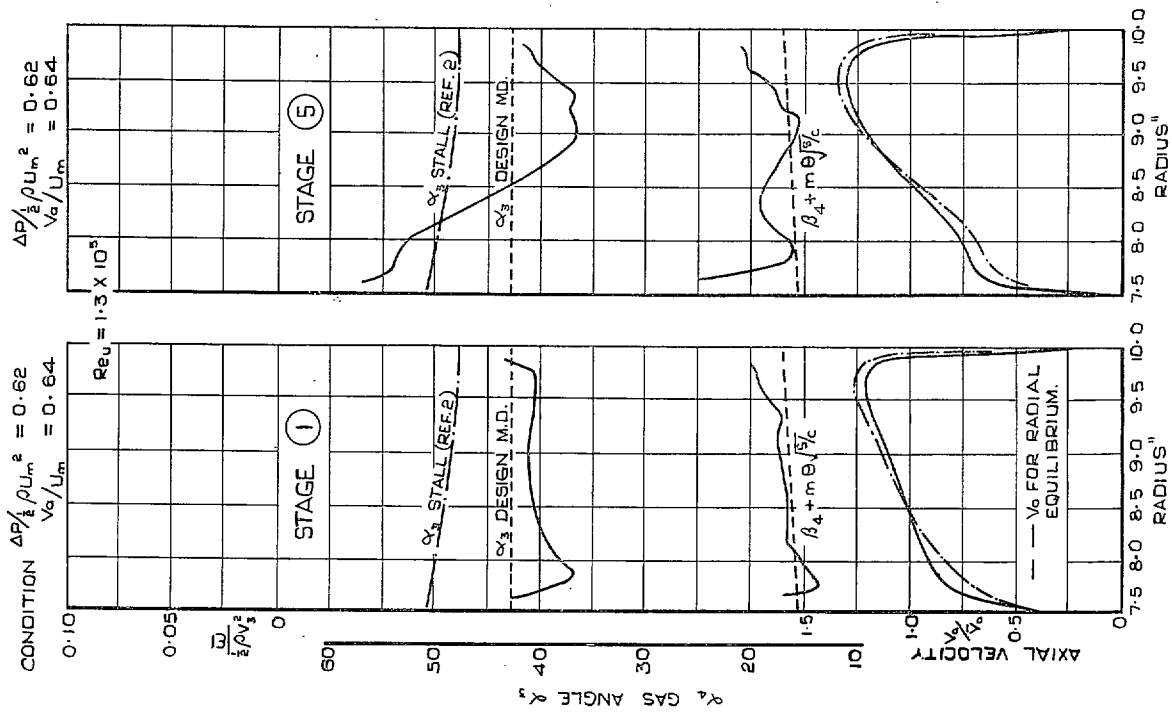

FIG. 11. Untwisted constant section blades.

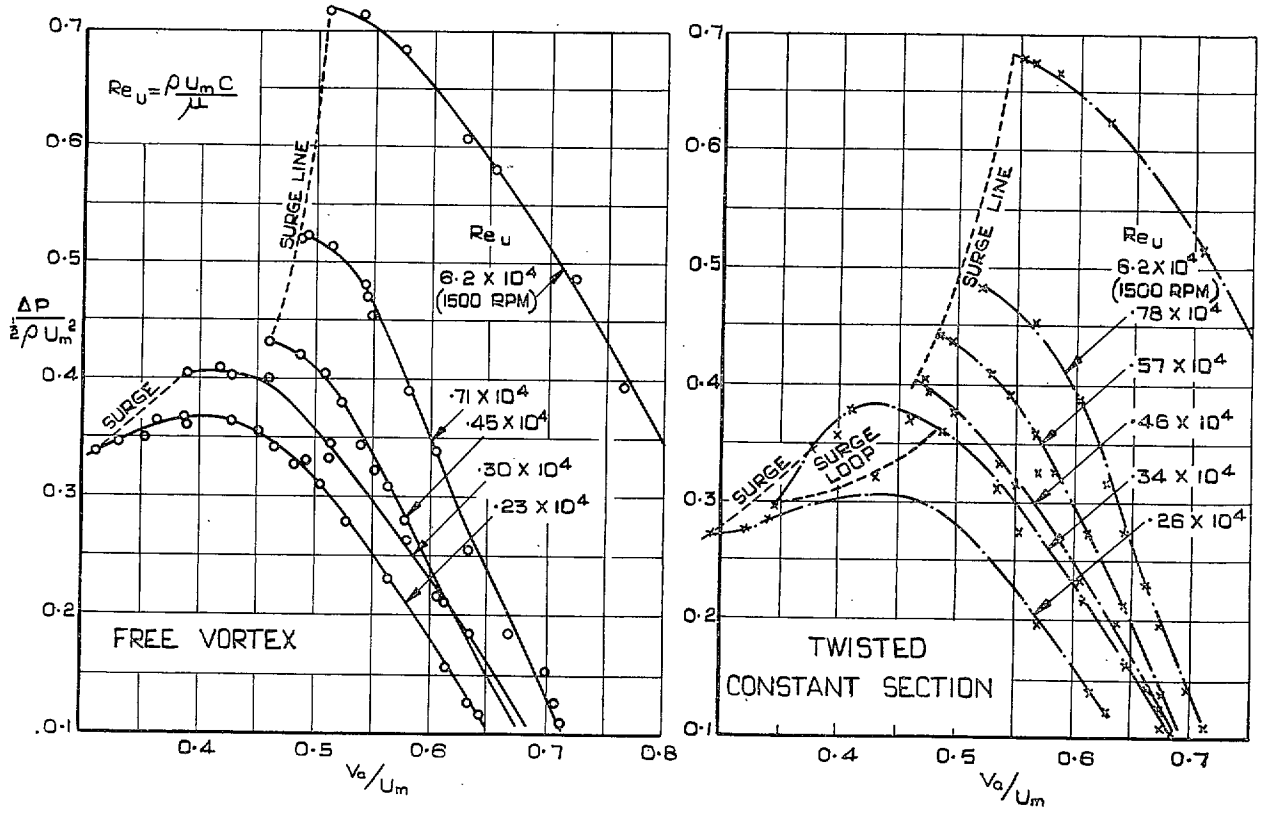

FIG. 12. Reynolds number effect on non-dimensional pressure coefficient.

J4351 Wt.19/8411 K7 4/56 D&Co. 34/263

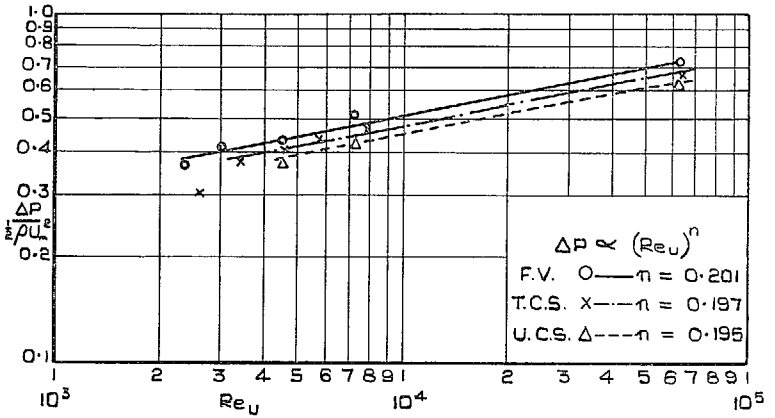

THE EFFECT OF REYNOLDS NUMBER ON MAXIMUM PRESSURE COEFFICIENT.

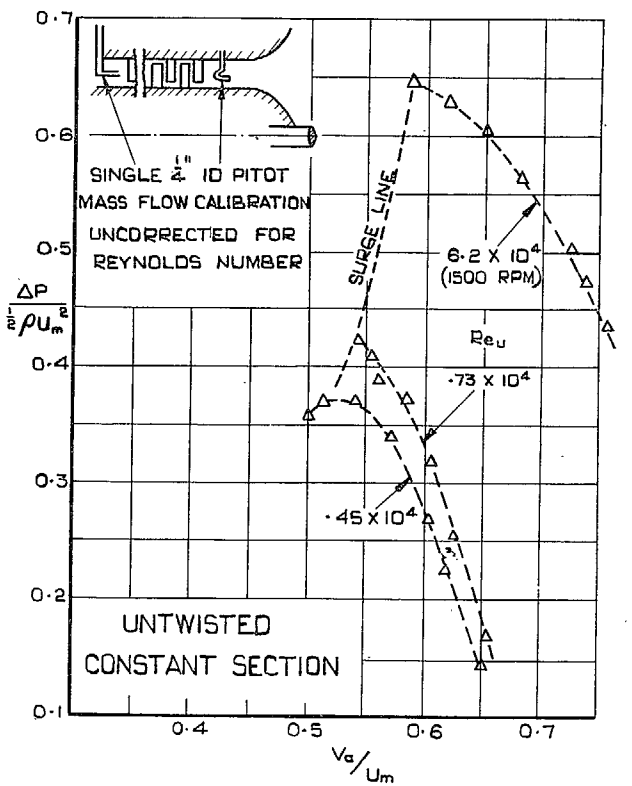

FIG. 13. Reynolds number effect on non-dimensional pressure coefficient.

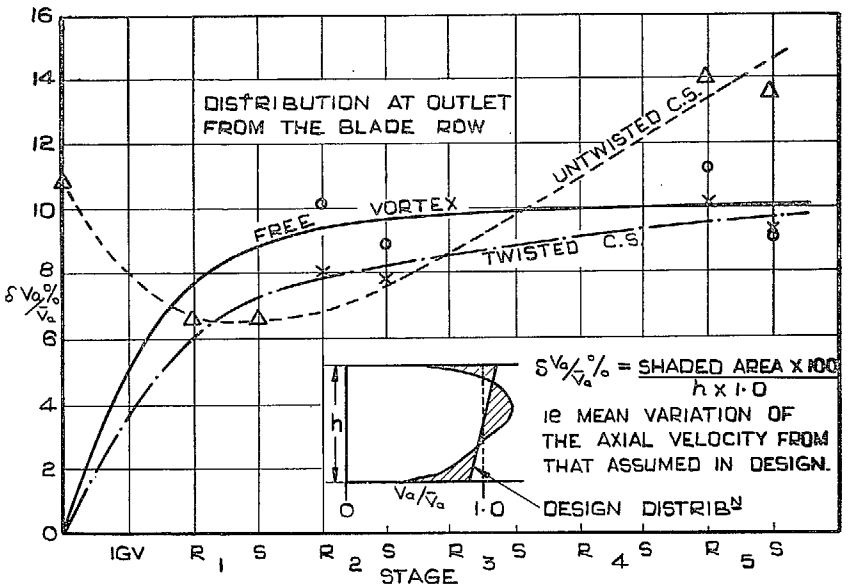

Variation of axial velocity profile.

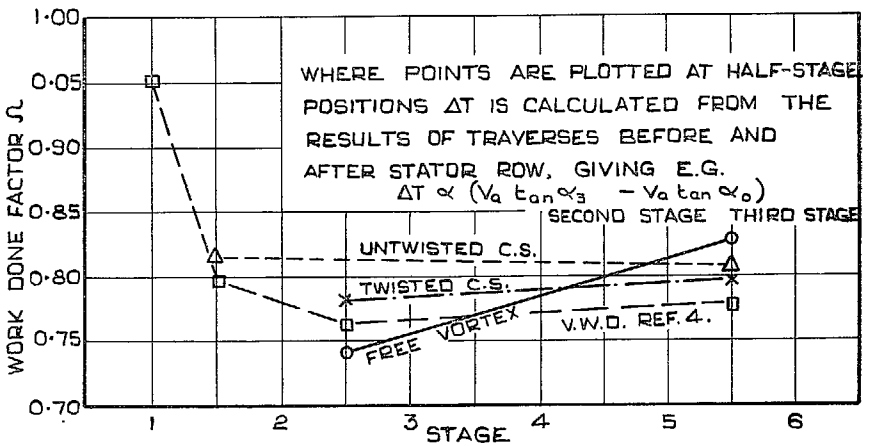

Variation of work-done factor.

FIG. 14.

PRINTED IN GREAT BRITAIN

Publications of the Aeronautical Research Council

ANNUAL TECHNICAL REPORTS OF THE AERONAUTICAL RESEARCH COUNCIL (BOUND VOLUMES)

1938 Vol. I. Aerodynamics General, Performance, Airscrews. 50*s.* (51*s.* 8*d.*)
Vol. II. Stability and Control, Flutter, Structures, Seaplanes, Wind Tunnels, Materials. 30*s.* (31*s.* 8*d.*)

1939 Vol. I. Aerodynamics General, Performance, Airscrews, Engines. 50*s.* (51*s.* 8*d.*)
Vol. II. Stability and Control, Flutter and Vibration, Instruments, Structures, Seaplanes, etc. 63*s.* (64*s.* 8*d.*)

1940 Aero and Hydrodynamics, Aerofoils, Airscrews, Engines, Flutter, Icing, Stability and Control, Structures, and a miscellaneous section. 50*s.* (51*s.* 8*d.*)

1941 Aero and Hydrodynamics, Aerofoils, Airscrews, Engines, Flutter, Stability and Control, Structures. 63*s.* (64*s.* 8*d.*)

1942 Vol. I. Aero and Hydrodynamics, Aerofoils, Airscrews, Engines. 75*s.* (76*s.* 8*d.*)
Vol. II. Noise, Parachutes, Stability and Control, Structures, Vibration, Wind Tunnels. 47*s.* 6*d.* (49*s.* 2*d.*)

1943 Vol. I. Aerodynamics, Aerofoils, Airscrews. 80*s.* (81*s.* 8*d.*)
Vol. II. Engines, Flutter, Materials, Parachutes, Performance, Stability and Control, Structures. 90*s.* (91*s.* 11*d.*)

1944 Vol. I. Aero and Hydrodynamics, Aerofoils, Aircraft, Airscrews, Controls. 84*s.* (86*s.* 9*d.*)
Vol. II. Flutter and Vibration, Materials, Miscellaneous, Navigation, Parachutes, Performance, Plates and Panels, Stability, Structures, Test Equipment, Wind Tunnels. 84*s.* (86*s.* 9*d.*)

ANNUAL REPORTS OF THE AERONAUTICAL RESEARCH COUNCIL—

1933–34	1*s.* 6*d.* (1*s.* 8½*d.*)	1937	2*s.* (2*s.* 2½*d.*)
1934–35	1*s.* 6*d.* (1*s.* 8½*d.*)	1938	1*s.* 6*d.* (1*s.* 8½*d.*)
April 1, 1935 to Dec. 31, 1936	4*s.* (4*s.* 5½*d.*)	1939–48	3*s.* (3*s.* 3½*d.*)

INDEX TO ALL REPORTS AND MEMORANDA PUBLISHED IN THE ANNUAL TECHNICAL REPORTS, AND SEPARATELY—

April, 1950 – – – – – R. & M. No. 2600. 2*s.* 6*d.* (2*s.* 7½*d.*)

AUTHOR INDEX TO ALL REPORTS AND MEMORANDA OF THE AERONAUTICAL RESEARCH COUNCIL—

1909–January, 1954 – – – R. & M. No. 2570. 15*s.* (15*s.* 5½*d.*)

INDEXES TO THE TECHNICAL REPORTS OF THE AERONAUTICAL RESEARCH COUNCIL—

December 1, 1936 — June 30, 1939.	R. & M. No. 1850.	1*s.* 3*d.* (1*s.* 4½*d.*)
July 1, 1939 — June 30, 1945. –	R. & M. No. 1950.	1*s.* (1*s.* 1½*d.*)
July 1, 1945 — June 30, 1946. –	R. & M. No. 2050.	1*s.* (1*s.* 1½*d.*)
July 1, 1946 — December 31, 1946.	R. & M. No. 2150.	1*s.* 3*d.* (1*s.* 4½*d.*)
January 1, 1947 — June 30, 1947. –	R. & M. No. 2250.	1*s.* 3*d.* (1*s.* 4½*d.*)

PUBLISHED REPORTS AND MEMORANDA OF THE AERONAUTICAL RESEARCH COUNCIL—

Between Nos. 2251–2349. – –	R. & M. No. 2350.	1*s.* 9*d.* (1*s.* 10½*d.*)
Between Nos. 2351–2449. – –	R. & M. No. 2450.	2*s.* (2*s.* 1½*d.*)
Between Nos. 2451–2549. – –	R. & M. No. 2550.	2*s.* 6*d.* (2*s.* 7½*d.*)
Between Nos. 2551–2649. – –	R. & M. No. 2650.	2*s.* 6*d.* (2*s.* 7½*d.*)

Prices in brackets include postage

HER MAJESTY'S STATIONERY OFFICE

York House, Kingsway, London W.C.2; 423 Oxford Street, London W.1 (Post Orders: P.O. Box 569, London S.E.1); 13a Castle Street, Edinburgh 2; 39 King Street, Manchester 2; 2 Edmund Street, Birmingham 3; 109 St. Mary Street, Cardiff; Tower Lane, Bristol 1; 80 Chichester Street, Belfast, *or through any bookseller*

S.O. Code No. 23-2928